# Application of a multilevel Redfield theory to electron transfer in condensed phases

John M. Jean, Richard A. Friesner, and Graham R. Fleming

Citation: The Journal of Chemical Physics **96**, 5827 (1992); doi: 10.1063/1.462858
View online: http://dx.doi.org/10.1063/1.462858
View Table of Contents: http://scitation.aip.org/content/aip/journal/jcp/96/8?ver=pdfcov
Published by the AIP Publishing

# Application of a multilevel Redfield theory to electron transfer in condensed phases

John M. Jean
*Department of Chemistry, Washington University, St. Louis Missouri 63130*

Richard A. Friesner
*Department of Chemistry, Columbia University, New York, New York 10027*

Graham R. Fleming
*Department of Chemistry and The James Franck Institute, University of Chicago, Chicago, Illinois 60637*

(Received 23 October 1991; accepted 9 January 1992)

A quantum mechanical theory of photoinduced electron transfer, based on the Redfield theory of relaxation, is developed and applied to the standard two state–one mode system interacting with a thermal bath. Quantum mechanical treatment of the reaction coordinate allows incorporation of both finite vibrational dephasing and energy flow rates into the description of electron transfer dynamics. The field–matter interaction is treated explicitly to properly incorporate the total energy and magnitude of the vibrational coherence present in the initially prepared state. Calculation of the reduced density matrix of the system is carried out in a vibronic basis that diagonalizes the electron exchange coupling so that the method is valid for arbitrarily large coupling strength. For weak electronic coupling, we demonstrate the equivalence between the results from Redfield theory and those obtained from the standard perturbative expression (golden rule) for nonadiabatic electron transfer. We then discuss quantitatively the breakdown of the Fermi golden rule with increasing electronic coupling strength. The failure of the golden rule is seen to result from either slow energy equilibration in the reactant or product well or from quantum interference effects resulting from finite dephasing rates. For cases where the reorganization energy is large compared to the frequency of reactive motion, such that we may ignore nuclear tunneling, results from the theory show good agreement with those from the semiclassical Landau–Zener theory when motion of the reaction coordinate through the surface crossing region can be considered to be ballistic. Finally results are shown in the weak damping (coherent) limit that demonstrate interference effects between phase coherences involving states in both wells.

## I. INTRODUCTION

The theoretical description of electron transfer (ET) processes in condensed phases continues to be of interest in the chemical physics, biophysics, and condensed matter communities.[1-2] The standard picture of photoinduced ET involves the coupling of two electronically excited states, a neutral state and a charge transfer state, to a single nuclear degree of freedom, i.e., the reaction coordinate. This coordinate may be collective in nature, such as the solvent polarization, or correspond to a specific vibrational motion of a protein or lattice. The electronic interaction gives rise to a splitting of the energy levels in the region where the neutral and charge transfer potential energy surfaces intersect. The diabatic and adiabatic surfaces for the standard model are shown in Fig. 1. These one-dimensional surfaces represent a reduced picture for the ET process in which the reaction coordinate, which experiences strong vibronic coupling, is treated explicitly while the vast majority of nuclear degrees of freedom, which are only weakly coupled to the electronic states, constitute a thermal bath. The coupling between the system and bath degrees of freedom introduces dissipation into the system.

Standard theoretical treatments of ET assume that a separation of timescales exists between the fast dissipative processes in the system and the intrinsic time scale of the electron tunneling process, given by the inverse of the electronic coupling matrix element. It is useful to distinguish two types of dissipation, energy flow between the reaction coordinate and the bath and the destruction of phase coherences between quantum states. These two processes have different physical origins and manifest themselves in different ways experimentally. The former arises from inelastic interactions with the bath and results in vibrational population relaxation on a timescale denoted by $T_1$. The latter process, pure dephasing, arises from quasielastic interactions that leave the state of the system unchanged but lead to a change in phase of the wave function. The timescale of this process is denoted by $T_2^*$. Both processes contribute to the total dephasing rate for any pair of quantum levels. Numerous time- and frequency-domain techniques have been devised in recent years to provide information about vibrational and electronic dephasing rates for molecules in condensed phase environments.[13,14] For moderate to large molecules these range from subpicosecond to several picoseconds and generally depend strongly on temperature.

The complete loss of phase coherence on a sufficiently short timescale allows the ET process to be treated by classical or semiclassical methods such as those of Marcus[3] and Landau and Zener.[1,15-17] The semiclassical Landau–Zener

 0021-9606/92/085827-16$06.00  

theory, or surface "hopping" approach, treats the nuclear motion classically. Quantum mechanics enters only at the configuration where the diabatic potential surfaces cross. At this point, the probability of the electron tunneling to the product surface is computed via the Schrödinger equation.

For cases where phase coherence is unimportant, two important limiting cases for the dynamics can be discerned. If the electronic coupling is weak, the probability of hopping to the product surface at the crossing point is small, and the crossing region will be sampled many times before an electronic state change will occur. The rate constant for electron transfer in this case depends on the magnitude of the electronic coupling and the process is said to be nonadiabatic. In the limit of very weak coupling, the golden rule of perturbation theory provides a connection between quantum mechanics and chemical rate processes. This approach forms the basis of radiationless transition theories and has been extended to nonadiabatic electron transfer by Jortner and others.[18,19] In the other extreme, the adiabatic limit, the splitting between surfaces is large in the crossing region, the probability of the electron tunneling to the product state at the crossing point approaches unity, and nuclear motion becomes rate limiting. In this limit classical models based on the escape of a particle over a potential barrier subject to frictional forces are applicable.[7,20]

When the dephasing rates in the reactant and product manifolds become comparable to the time scale associated with electron tunneling, the semiclassical description is no longer valid and the nuclear motion must be treated quantum mechanically. In this regime, the initially excited neutral state does not equilibrate before reaction occurs and we must take into account the nature of the optically prepared state. Optical excitation, in addition to creating population in one or more vibrational levels, can result in the creation of phase coherences involving vibronic levels in both the ground and excited states. Coherences between ground and excited state levels (i.e., optical coherences) generally decay on an exceedingly rapid timescale, which for large molecules in solution can be as short as sub-100 fs. If the excitation pulse is sufficiently short, the large spectral bandwidth can lead to coherent excitation of several vibrational states within the excited state manifold resulting in a vibrational coherence that will oscillate at the well frequency. When the destruction of this coherence occurs on a sufficiently long timescale, the ET process can no longer be considered a rate process, and quantum effects arising from the preservation of phase relationships between different quantum states can give rise to complicated dynamical behavior that contains a wealth of information on the nature and strength of the various types of coupling present in the system.

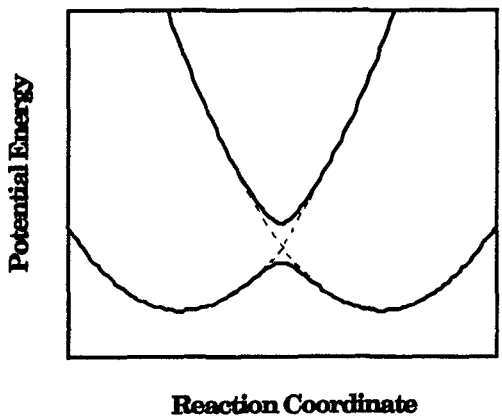


FIG. 1. Diabatic (– – –) and adiabatic (—) potential energy surfaces for electron transfer.

The importance of electron transfer in many biologically and technologically important areas has lead to intense experimental activity in recent years. Much of this attention has been focused on fundamental events in photosynthesis.[21–25] Ultrafast spectroscopic studies have shown that the transfer of an electron in the primary step occurs on a picosecond or subpicoseond timescale depending on the temperature. Simple theoretical estimates of electronic coupling strengths between neighboring pigments in various photosynthetic systems based on x-ray crystal structures have yielded interaction energies in the 10–200 $cm^{-1}$ range.[26] The timescales associated with coupling strengths this large are comparable to those associated with dephasing in large molecules which suggests that quantum phase effects may play an important role in the dynamics of these processes, particularly at low temperatures where dephasing times can be long.

The interpretation of experiments on ultrafast electron transfer and other photophysical processes, such as excitation transfer, requires a theoretical approach that is capable of treating the reactive processes and dissipative processes explicitly. In the present work we develop a density operator approach based on the Redfield theory of relaxation which has found wide application in the field of magnetic resonance,[27,28] and, to a lesser extent, optical spectroscopy.[29] Though the method is applicable to a number of photochemical and photophysical processes, we develop the formalism in the context of photoinduced electron transfer. This work derives, at least in part, from the work of Wertheimer and Silbey[30] on the dynamics of triplet states in naphthalene dimers. The theory is based on a microscopic model for the interaction between system and bath degrees of freedom and is nonperturbative in the electronic coupling allowing us to interpolate between various limits involving slow and fast dissipation. Those nuclear degrees of freedom that experience strong vibronic interactions are treated quantum mechanically which allows proper incorporation of vibrational relaxation and dephasing processes. A great deal of work has appeared in the past ten or fifteen years devoted to developing a firm microscopic understanding of dephasing processes in large molecules in solids and solutions at infinite dilution. Very little, however, has been done to incorporate these ideas into a quantum theory of condensed phase reaction dynamics. The multilevel Redfield theory described here should be seen as our initial attempt in this direction.

The rest of this paper is organized as follows: In Sec. II we provide a detailed description of the formalism and present the strategy for numerical solution of the Redfield equations of motion for the elements of the reduced density matrix for the system. In Sec. III we demonstrate the

equivalence of our approach and the golden rule and semiclassical theories in the appropriate limits. In addition we present a quantitative discussion of the breakdown of the golden rule formula starting from the diabatic representation for the system electronic states. We conclude this section by showing simulation results in the weak damping limit where coherence effects are important. Concluding remarks are contained in Sec. IV.

## II. THEORY

### A. System Hamiltonian

In this section we develop the formal aspects of a multilevel Redfield theory in the context of a simple model for photoinduced electron transfer. The model consists of a ground state and two excited manifolds, a neutral ($N$) state and a charge transfer (CT) state, coupled to a single nuclear coordinate, which is in turn weakly coupled to a large number of nuclear degrees of freedom that constitute a thermal bath. We include a system–field interaction that couples the ground and $N$ states via the radiation field. The inclusion of the ground state and field interaction is in contrast to previous treatments of electron transfer; however, we shall see that in cases where the electronic process competes effectively with vibrational relaxation processes, the nature of the initial optically excited state will influence the subsequent dynamical behavior. The vibronic population distribution in the initially excited state as well as the magnitude of the initial vibrational coherence is determined by the displacement of the excited state potential surface relative to that of the ground state (i.e., through the Franck–Condon principle) and the spectral and temporal properties of the excitation source.

We distinguish between the system nuclear coordinate, which experiences strong vibronic coupling, and the remaining modes that form the bath. We denote the former by $Q$ and the latter by $\mathbf{q}$. For now we neglect the ground state and system–field Hamiltonians and develop the form of the Hamiltonian for the $N$ and CT manifolds. In terms of the diabatic (site) states $N$ and CT, the Hamiltonian can be written as

$$\mathscr{H}_i = \mathscr{H}_N(\mathbf{q},Q)|N\rangle\langle N| + \mathscr{H}_{CT}(\mathbf{q},Q)|CT\rangle\langle CT| + \mathscr{J}(\mathbf{q},Q)\{|N\rangle\langle CT| + |CT\rangle\langle N|\}. \quad (1)$$

The electronic degrees of freedom have been written in terms of projection operators for the diabatic states. $\mathscr{J}(\mathbf{q},Q)$ is the electronic coupling (exchange) term that describes the electronic tunneling process between reactant and product states. The vibrational Hamiltonians, $\mathscr{H}_i(\mathbf{q},Q)$, are multidimensional operators that describe the static and dynamic properties of the uncoupled diabatic states. We can formally reduce these to one-dimensional effective Hamiltonians by defining a new set of operators that represent canonical averages over the bath modes. Let

$$H_i(Q) = \langle \mathscr{H}_i(\mathbf{q},Q)\rangle, \quad (2a)$$

$$J(Q) = \langle \mathscr{J}(\mathbf{q},Q)\rangle. \quad (2b)$$

In terms of these bath-averaged operators, the Hamiltonian for the electronically excited states is

$$H_e = [H_N(Q) + V_N(\mathbf{q},Q)]|N\rangle\langle N| + [H_{CT}(Q) + V_{CT}(\mathbf{q},Q)]|CT\rangle\langle CT| + [J(Q) + V_{N,CT}(\mathbf{q},Q)]\{|N\rangle\langle CT| + |CT\rangle\langle N|\}, \quad (3)$$

where $V_i(\mathbf{q},Q) = \mathscr{H}_i(\mathbf{q},Q) - H_i(Q)$ and $V_{N,CT}(\mathbf{q},Q) = \mathscr{J}(\mathbf{q},Q) - J(Q)$ represent fluctuations of these operators from their canonical averages. From here on we neglect fluctuations that are off-diagonal in the electronic index and concentrate on the site fluctuations, which give rise to dissipation within a diabatic state.

The total Hamiltonian can be expressed as a sum of system, bath, system–bath, and system–field terms.

$$H = H_S + H_B + H_{SB} + H_{SF} \quad (4)$$

with

$$H_S = H_G + H_e = H_G(Q)|G\rangle\langle G| + H_N(Q)|N\rangle\langle N| + H_{CT}(Q)|CT\rangle\langle CT| + J(Q)\{|N\rangle\langle CT| + |CT\rangle\langle N|\}, \quad (5a)$$

$$H_{SB} = V_N(\mathbf{q},Q)|N\rangle\langle N| + V_{CT}(\mathbf{q},Q)|CT\rangle\langle CT|, \quad (5b)$$

$$H_{SF}(t) = -\mu_{G,N}\{|G\rangle\langle N| + |N\rangle\langle G|\}\cdot E(t), \quad (5c)$$

where $\mu_{G,N} = \langle G|\hat{\mu}|N\rangle$ is the transition dipole matrix element for the $G\rightarrow N$ transition and $E(t)$ is the time-dependent electric field.

We have chosen the reaction coordinate $Q$ such that its origin corresponds to the equilibrium position of the ground state surface. In dimensionless units ($Q = \sqrt{m\omega/\hbar}\,Q'$, $P = (\sqrt{m\hbar\omega})^{-1}P'$; $Q'$ is the actual coordinate and $P'$ its conjugate momentum), the ground state vibrational Hamiltonian is

$$H_G(Q) = \hbar\omega(P^2/2 + Q^2/2). \quad (6)$$

We assume the excited state surfaces differ by only linear displacements from the ground state. Then

$$H_N(Q) = \hbar\omega P^2/2 + 1/2\hbar\omega(Q - \Delta_N)^2 + \epsilon_N, \quad (7a)$$

$$H_{CT}(Q) = \hbar\omega P^2/2 + 1/2\hbar\omega(Q - \Delta_{CT})^2 + \epsilon_{CT}, \quad (7b)$$

where $\Delta_i$ is the position of the minimum of excited state $i$ and $\epsilon_i$ is the zeroth-order energy separation between the $i$th excited state surface and the ground state surface. Inclusion of higher order terms (frequency shifts, anharmonicities) is straightforward, however truncation at the linear term is in accord with previous treatments of the double well problem.[31]

Further progress is facilitated by transforming the Hamiltonian to the occupation number representation. Making the replacement $Q\rightarrow(a + a^\dagger)/\sqrt{2}$ and $P\rightarrow -i(a - a^\dagger)/\sqrt{2}$ where $a^\dagger, a$ are the usual boson operators and defining the zero of energy to be the bottom of the ground state well, the system Hamiltonian becomes

$$H_s = (a^\dagger a + 1/2)\hbar\omega|G\rangle\langle G| + [\epsilon_N + (a^\dagger a + 1/2)\hbar\omega + g_N(a + a^\dagger)]|N\rangle\langle N| + [\epsilon_{CT} + (a^\dagger a + 1/2)\hbar\omega + g_{CT}(a + a^\dagger)] \times |CT\rangle\langle CT| + J(Q)[|N\rangle\langle CT| + |CT\rangle\langle N|], \quad (8)$$

where the $g_i$ are linear coupling parameters ($g_i = -\Delta_i\hbar\omega/\sqrt{2}$). The $0\rightarrow 0$ transition for the $G\rightarrow i$ electronic transition is given by $E_i^{0-0} = \epsilon_i - g_i^2/\omega$. For the electron transfer process, the reorganization energy associated with the reaction coordinate is given by

$$E_r = (g_N - g_{CT})^2/\hbar\omega, \tag{9a}$$

and the energy bias between the states (i.e., free energy of reaction) is

$$\epsilon_{bias} = E_{CT}^{0-0} - E_N^{0-0}. \tag{9b}$$

For the remainder of this paper we assume the Condon approximation is valid, that is the exchange coupling matrix element $J$ is independent of the nuclear coordinate $Q$. Inclusion of non-Condon effects, however, poses no difficulty.

In the next section we develop the form of the operator that introduces vibrational relaxation processes into our picture. The various interactions with the bath will turn out to be level specific, thus it is convenient to express the system Hamiltonian in terms of vibronic operators that expose this level dependence. Adopting a direct product basis for the vibronic states with greek letters denoting vibrational quantum number, the vibronic operators are of the form

$$\mathscr{P}_{i\alpha j\beta} = |i,\alpha\rangle\langle j,\beta|. \tag{10}$$

The system Hamiltonian becomes

$$H_S = \sum_{ij}\sum_{\alpha\beta}\epsilon_{i\alpha,j\beta}\mathscr{P}_{i\alpha j\beta}, \tag{11}$$

where $\epsilon_{i\alpha,j\beta}$ are matrix elements of the excited state Hamiltonian in the ground state basis.

### B. Derivation of the fluctuation operator

In the previous section we discussed an effective Hamiltonian for the static properties of the system. If the system is prepared initially in one of the diabatic states, the electron exchange interaction will give rise to coherent (reversible) electron transfer between states. To introduce irreversibility into this picture we need to take into account the fluctuating terms in the Hamiltonian. The system–bath interaction for diabatic state $|i\rangle$ was shown in the previous section to be $V_i(\mathbf{q},Q) = \mathscr{H}_i(\mathbf{q},Q) - \langle\mathscr{H}_i(\mathbf{q},Q)\rangle_{bath}$. Expanding this to second order in the system coordinate about the equilibrium position of state $i(\Delta_i)$ gives

$$V_i(\mathbf{q},Q) = V_i(\mathbf{q},\Delta_i) + (\partial V_i(\mathbf{q},Q)/\partial Q)_{\Delta_i}(Q-\Delta_i) + 1/2(\partial^2 V_i(\mathbf{q},Q)/\partial Q^2)_{\Delta_i}(Q-\Delta_i)^2. \tag{12}$$

The zeroth-order terms do not depend on $Q$ and are thus included in the bath Hamiltonian. We can simplify this expression by making the following substitutions

$$f_i^{(1)}(\mathbf{q}) = (\partial V_i(\mathbf{q},Q)/\partial Q)_{\Delta_i}, \tag{13a}$$

$$f_i^{(2)}(\mathbf{q}) = 1/2(\partial^2 V_i(\mathbf{q},Q)/\partial Q^2)_{\Delta_i}. \tag{13b}$$

These are fluctuation operators for the site states and depend only on the bath degrees of freedom.

The vibrational relaxation processes we are interested in occur in the excited state manifolds, so it is most convenient to express the operators that give rise to these processes in terms of the vibrational states belonging to the particular electronic state $|i\rangle$. These are states that diagonalize the linear coupling terms, $g_i$, in the Hamiltonian. These displaced oscillator states will be denoted by greek letters with a prime.

In terms of the displaced oscillator states, the operator describing the system–bath interaction becomes

$$H_{SB} = \sum_{ij}\sum_{\alpha'\beta'}\delta_{ij}\phi_{\alpha'\beta'}^{(i)}\mathscr{P}_{i\alpha' j\beta'}, \tag{14}$$

where $\phi_{\alpha'\beta'}^{(i)} = \langle\alpha'|V_i(\mathbf{q},Q)|\beta'\rangle$ are elements of the fluctuation matrix for the diabatic state $|i\rangle$. The matrix elements are easily calculated using the properties of the boson creation and annihilation operators.

$$\phi_{\alpha'\beta'}^{(i)} = f_i^{(1)}\sqrt{\beta'}\,\delta_{\alpha',\beta'-1} + f_i^{(1)}\sqrt{\beta'+1}\,\delta_{\alpha',\beta'+1} + f_i^{(2)}\beta'\delta_{\alpha',\beta'}. \tag{15}$$

The first two terms gives rise to one quantum vibrational energy relaxation while the third term connects a state with itself and describes a pure dephasing process. We will neglect two-phonon relaxation processes.

### C. Vibrational relaxation and pure dephasing in the site representation

With the bath described by the diagonal ($f_i^{(2)}$) and off-diagonal ($f_i^{(1)}$) fluctuation operators, it is a simple matter to calculate the various relaxation rates which represent convenient parameters to use in formulating a picture of ET in systems that experience strong electronic coupling. The advantage of expressing these parameters in the uncoupled (diabatic) representation is that they can be easily related to experimental measurements on uncoupled donor and acceptor species.

Assuming the coupling between the reaction coordinate and the bath is sufficiently weak, the rate constant, $\Gamma_{\alpha'\beta'}$, for population relaxation from vibrational state $\alpha'$ to $\beta'$ can be written as a Fourier transform of the autocorrelation function of the appropriate fluctuation matrix elements[32,33]

$$\Gamma_{\alpha'\beta'}^{(i)} = 1/T_1 = h^{-2}\int_{-\infty}^{+\infty} dt\, e^{i\omega_{\alpha'\beta'}t}\langle\phi_{\alpha'\beta'}^{(i)}(t)\phi_{\beta'\alpha'}^{(i)}(0)\rangle, \tag{16}$$

where $\phi_{\alpha'\beta'}(t) = \exp(iH_B t)\phi_{\alpha'\beta'}(0)\exp(-iH_B t)$. Only the off-diagonal fluctuations contribute to this process, so, in terms of the $f_i^{(1)}$

$$\Gamma_{\alpha'\beta'}^{(i)} = h^{-2}|\langle\alpha'|Q|\beta'\rangle|^2\int_{-\infty}^{+\infty} dt\, e^{i\omega_{\alpha'\beta'}t}\langle f_i^{(1)}(t)f_i^{(1)}(0)\rangle. \tag{17}$$

The correlation function appearing in Eq. (17) involves only the bath variables and is assumed to decay exponentially with a time constant $\tau_c$, the bath correlation time. In the motionally narrowed limit, $\langle f_i^{(2)}\rangle\tau_c \ll 1$, the rate constant for the process $\alpha'\rightarrow\beta'$ in site state $i$ is thus

$$\Gamma_{\alpha'\beta'}^{(i)} = \alpha' f_i^{(1)2}\tau_c \tag{18}$$

which scales linearly with the vibrational quantum number. Detailed balance requires that the ratio of the two rates be given by the corresponding Boltzmann factor. Thus to en-

sure that the system relax to a Boltzmann distribution at long times, we force the rates to obey the detailed balance condition. The rate constant for the reverse process, transfer from $\beta'$ to $\alpha'$ is then

$$\Gamma_{\beta'\alpha'} = \exp(-\hbar\omega_{\alpha'\beta'}/kT)\Gamma_{\alpha'\beta'}. \tag{19}$$

Coherent excitation of two (or more) vibrational levels in the initially excited electronic state results in a phase coherence between the states which gives rise to a macroscopic vibrational amplitude. This amplitude can be written as

$$\langle Q(t)\rangle = \mathrm{Tr}\{\rho(t)Q\}, \tag{20}$$

where $\rho(t)$ is the time-dependent density matrix for the vibrational states. For a two-level system,

$$\langle Q(t)\rangle = \rho_{\alpha'\beta'}(t)Q_{\beta'\alpha'} + \rho_{\beta'\alpha'}(t)Q_{\alpha'\beta'}. \tag{21}$$

In the absence of population relaxation, the phase coherence described by $\rho_{\alpha'\beta'}(t)$ will, in the Bloch approximation, decay exponentially with time constant $T_2^*$. Again, perturbation theory gives the result

$$\begin{aligned}\Gamma^*_{\beta'\alpha'} &= 1/T_2^{\alpha'\beta'*} \\ &= \hbar^{-2}/2\int_{-\infty}^{+\infty} dt\,\langle(\phi_{\alpha'\alpha'}(t) - \phi_{\beta'\beta'}(t)) \\ &\quad\times(\phi_{\alpha'\alpha'}(0) - \phi_{\beta'\beta'}(0))\rangle.\end{aligned} \tag{22}$$

The total dephasing rate between two levels is given by

$$\Gamma_{\alpha'\beta'} = \sum_{\gamma}\Gamma_{\alpha'\gamma} + \sum_{\gamma}\Gamma_{\beta'\gamma} + \Gamma^*_{\beta'\alpha'}. \tag{23}$$

where the summations denote the sum of all the $T_1$ processes originating in states $\alpha'$ and $\beta'$.

### D. System–field interaction

In conventional electron transfer theories for excited states, the assumption of fast dissipation results in dynamics that are insensitive to the nature of the optically prepared state. For cases where either population relaxation and/or pure dephasing occurs on a timescale comparable to the electron transfer, this is not necessarily true. In these cases we must explicitly take into account the frequency and temporal properties of the excitation pulse and the Franck–Condon factors for the relevant optical transitions. The interaction between the system and an incoming laser pulse is given by

$$H_{SF}(t) = -\mu\cdot E(t), \tag{24}$$

where $\mu$ is the transition dipole operator and $E(t)$ is the time-dependent electric field, which can be written as

$$E(t) = E_0(t)\{\exp(i\omega_L t) + \exp(-i\omega_L t)\}, \tag{25}$$

where $E_0(t)$ is the temporal profile of the pulse and $\omega_L$ the center frequency. Assuming the excitation pulse is a transform limited pulse from a mode-locked laser, the spectral width is determined by the Fourier transform of $E_0(t)$.

We assume only the neutral state is optically accessible from the ground state, so that the transition dipole operator has the form

$$\mu = \sum_{\alpha\alpha'}\mu_{N\alpha',G\alpha}\{|N,\alpha'\rangle\langle G,\alpha| + |G,\alpha\rangle\langle N,\alpha'|\}, \tag{26}$$

where $\alpha$ and $\alpha'$ refer to vibrational levels associated with the ground ($G$) and nuetral ($N$) excited states, respectively. The matrix elements of the transition dipole operator have the form

$$\mu_{N\alpha',G\alpha} = \langle N|\hat{\mu}|G\rangle\langle\alpha'|\alpha\rangle. \tag{27}$$

Without loss of generality, we set the electronic matrix element equal to one. The vibrational overlaps, $\langle\alpha'|\alpha\rangle$, depend on the relative displacement of the $G$ and $N$ states.

### E. Density operator for the system

We can summarize the previous sections by writing down the full Hamiltonian in terms of the vibronic operators.

$$\begin{aligned}H = &\sum_{ij}\sum_{\alpha\beta}\{\epsilon_{i\alpha,j\beta} + \delta_{ij}\phi_{\alpha\beta}\}\mathscr{P}_{i\alpha,j\beta} \\ &+ \sum_{\alpha\alpha'}\mu_{N\alpha',G\alpha}\{\mathscr{P}_{G\alpha,N\alpha'} + \mathscr{P}_{N\alpha',G\alpha}\}\cdot E(t) + H_B,\end{aligned} \tag{28}$$

where $\epsilon_{i\alpha,j\beta}$ is a matrix element of the excited state Hamiltonian in the ground state basis. The matrix elements of the fluctuation operator in the ground state vibrational basis are given by

$$\langle\alpha|\phi|\beta\rangle = \sum_{\alpha'\beta'} C^{(i)}_{\alpha\alpha'}C^{*(i)}_{\beta\beta'}\langle\alpha'|\phi|\beta'\rangle, \tag{30}$$

where $C^{(i)}_{\gamma\gamma'} = \langle\gamma|\gamma'\rangle$.

To properly treat both the coherent motion and relaxation processes, we must solve for the reduced density matrix of the system $\mathbf{p}$, which represents a canonical average over the bath degrees of freedom.

$$p_{i\alpha,j\beta} = \mathrm{Tr}_B\{\mathbf{p}_B\mathscr{P}_{i\alpha,j\beta}\}/\mathrm{Tr}_B\{\mathbf{p}_B\}, \tag{31}$$

where $\mathbf{p}_B$ is the density matrix for the bath. Terms diagonal in both the electronic and vibrational indices correspond to populations of site vibrational states. Vibrational coherences are described by terms that are off-diagonal in the vibrational index. Terms that are off-diagonal in the electronic index correspond to electronic coherences between vibronic states in different wells.

The time dependence of the reduced density matrix for the excited states is governed by the quantum Liouville equation

$$\dot{\mathbf{p}}(t) = -i[\mathbf{H}_e,\mathbf{p}(t)] + \mathbf{R}\cdot\mathbf{p}(t). \tag{32}$$

The terms that give rise to dissipation are contained in the Redfield tensor $\mathbf{R}$. Before discussing the form of the $R$ tensor, it is convenient to transform to a representation in which the electronically excited Hamiltonian is diagonal and develop the relaxation equations in this basis.

### F. Transformation to the eigenstate representation

Theoretical treatments based on perturbation theory are valid for treating electron transfer between site states when the electronic coupling term $J$ is small. In order to develop a theoretical method that interpolates between the strong and weak coupling limits, it is convenient to work in a basis in which the electronic coupling is diagonal. The excited state

Hamiltonian in the ground state representation is given by

$$H_e = [\epsilon_N + (a^\dagger a + 1/2)\hbar\omega + g_N(a + a^\dagger)]|N\rangle\langle N| + [\epsilon_{CT} + (a^\dagger a + 1/2)\hbar\omega + g_{CT}(a + a^\dagger)] \times |CT\rangle\langle CT| + J[|N\rangle\langle CT| + |CT\rangle\langle N|]. \quad (33)$$

The matrix representation of this operator in the ground state representation is given by the $\epsilon$ matrix. If $\mathbf{U_{eg}}$ is the eigenvector matrix of $H_e$, then we can write

$$\mathbf{U_{eg}^\dagger \epsilon U_{eg}} = \mathbf{E}, \quad (34a)$$

$$\mathbf{U_{eg}^\dagger p U_{eg}} = \boldsymbol{\rho}, \quad (34b)$$

where $\mathbf{E}$ is the diagonal matrix of the system energies and $\boldsymbol{\rho}$ is the reduced density matrix in the eigenstate representation. $\mathbf{U_{eg}}$ is the transformation matrix for the ground and eigenstate represenations. We must also transform the fluctuation matrix $\phi$ to the eigenstate representation, however, care must be taken because, as mentioned above, the fluctuation matrix was originally set up in the representation that diagonalizes the excited state Hamiltonian in the absence of the electronic coupling, but with the vibronic parameters $g_N$ and $g_{CT}$ turned on. Thus the transformation of $\phi$ to the eigenstate representation can be written

$$\mathbf{U_{ge}^\dagger U_{gd}\, \boldsymbol{\phi}\, U_{gd}^\dagger U_{ge}} = \boldsymbol{\psi}, \quad (34c)$$

where $\mathbf{U_{gd}}$ denotes the transformation matrix between the ground state and diplaced oscillator representations.

We have thus transformed the problem of two manifolds undergoing relaxation in the presence of coherent electron exchange between localized states to a problem involving relaxation and dephasing processes involving a single manifold of states that are delocalized over the donor and acceptor.

## G. Dynamical calculations

### 1. Redfield equations

In the eigenstate representation, the site states are strongly mixed and it is convenient to use a notation in which only one index denotes a vibronic state. Assuming the total density matrix at $t=0$ can be written $\sigma(0) = \rho(0)\rho_B$, where the bath density operator is given by $\rho_B = \exp(-\beta H_B/\mathrm{Tr}(-\beta H_B))$, the density matrix elements in the eigenstate representation obey the equations of motion[34]

$$\dot{\rho}_{NM}(t) = -i\omega_{NM}\rho_{NM}(t) - \sum_{PQ} R_{NM,PQ}\rho_{PQ}(t), \quad (35)$$

where $\omega_{NM} = (E_N - E_M)/\hbar$ is the frequency of oscillation of the coherence between eigenstates $N$ and $M$. The Redfield approximation involves treating the fluctuations $\psi$ to second order. The $\mathbf{R}$ tensor elements have the following form:[34]

$$R_{NM,PQ} = h^{-2}\int_0^\infty dt \Big[\langle\psi_{QM}\psi_{NP}(t)\rangle\exp(-i\omega_{QM}(t) + \langle\psi_{QM}(t)\psi_{NP}\rangle\exp(-i\omega_{NP}t) - \delta_{QM}\sum_S \langle\psi_{NS}(t)\psi_{SP}\rangle\exp(-i\omega_{SP}t) - \delta_{PN}\sum_S\langle\psi_{QS}\psi_{SM}(t)\rangle\exp(-i\omega_{QS}t)\Big]. \quad (36a)$$

The correlation functions appearing in the above expression are assumed to decay exponentially with a correlation time $\tau_c$. If we assume that the bath correlation time is much shorter than any time scale on which the system evolves, we can replace the resulting Redfield tensor elements with their values at zero frequency. Carrying out the integration gives

$$R_{NM,PQ} = h^{-2}\tau_c\Big[2(\psi_{QM}\psi_{NP}) - \delta_{QM}\sum_s(\psi_{NS}\psi_{SP}) - \delta_{PN}\sum_S(\psi_{QS}\psi_{SM})\Big]. \quad (36b)$$

Elements of the Redfield tensor can thus be constructed from products of pairs of matrix elements of the fluctuation matrix in the eigenstate representation. In terms of our fluctuation parameters for the two wells, $f_i^{(1)}$ and $f_i^{(2)}$, a matrix element of $\psi$ can be written as

$$\psi_{NM} = \sum_i\sum_{\alpha\beta}\sum_{\alpha'\beta'} C^*_{i\alpha,N}C_{i\beta,N}C^{(i)}_{\alpha\alpha'}C^{*(i)}_{\beta\beta'}\big[f_i^{(1)}\{\sqrt{\beta'}\,\delta_{\alpha',\beta'-1} + [\sqrt{\beta'+1}\delta_{\alpha',\beta'+1}\} + f_i^{(2)}\delta_{\alpha',\beta'}, \quad (37)$$

where $C^*_{i\gamma,P}$ and $C^{(i)}_{\gamma\gamma'}$ are elements of the transformation matrices, $\mathbf{U_{ge}}$ and $\mathbf{U_{gd}}$, respectively. In Eq. (37) we have incorporated the correlation time into the definition of our fluctuation parameters $f$. That is, we have made the replacement $f_i \to f_i(\tau_c)^{1/2}$. Once again, as discussed in Sec. II C, invoking the Markov approximation ($\tau_c \to 0$) leads to a Redfield tensor that does not satisfy detailed balance. Thus, to ensure that the system relaxes to a Boltzmann distribution, we introduce the detailed balance condition in an *ad hoc* manner. Elements of the $\mathbf{R}$ tensor are, in general, complex, with the imaginary terms leading to a renormalization of the system frequencies. Note, however, that replacing the frequency-dependent $\mathbf{R}$ tensor with its value at zero frequency leads to a tensor that is real. The elements of the Redfield tensor have a straightforward interpretation. $R_{NM,PQ}$ is a rate constant for the process $\rho_{PQ} \to \rho_{NM}$. If $P=N$ and $Q=M$, this is a dephasing rate for the coherence $\rho_{PQ}$. If $P=Q$ and $N=M$, then the term represents a population relaxation rate between eigenstates $P$ and $N$. Other terms describe the coupling between populations and coherences and coherence transfer. The latter process will be important whenever the frequency mismatch $\omega_N - \omega_M - \omega_P + \omega_Q$ is within the width of the states.[27,35]

We rewrite Eq. (35) in a more compact form by defining the complex matrix $\mathbf{L}$, whose tensor elements are of the form

$$L_{NM,PQ} = \delta_{NP}\delta_{MQ}\omega_{NM} - iR_{NM,PQ}. \quad (38)$$

The equation of motion for the density matrix then becomes

$$\dot{\rho}(t) = i\mathbf{L}\rho(t), \quad (39)$$

which has the solution

$$\rho(t) = e^{i\mathbf{L}t}\rho(0). \quad (40)$$

### 2. Optical preparation of the initial state

For simplicity, we will assume there is no dissipation in the system during the excitation pulse. The validity of this approximation for any given pulse duration will obviously depend on the magnitude of the fluctuations. In the absence of dissipation, the dynamics of the density matrix is governed by the quantum mechanical Liouville equation

$$\rho(t) = -i/h\,[H_S + H_{SF}(t),\rho(t)], \tag{41}$$

where $H_{SF}(t) = -\mu\cdot E(t)$. Assuming the system–field interaction is weak, Eq. (38) can be solved perturbatively. The density operator, in the interaction representation, after an excitation pulse of duration $\tau$, is found, through second order, to be

$$\rho(\tau) = \rho(0) - i/\hbar \int_0^\tau dt\,[H'_{SF}(t),\rho(t)] - i/\hbar^2 \int_0^\tau dt \int_0^t dt'[H'_{SF}(t),[H'_{SF}(t'),\rho(t')]], \tag{42}$$

where $H'_{SF}(t)$ is $H_{SF}(t)$ in the interaction representation. Using the form of the transition dipole operator, Eq. (26), along with Eq. (42), and assuming the initial density operator is given by $\rho(0) = \Sigma p_\alpha |G\alpha\rangle\langle G\alpha|$, where $p_\alpha$ is the Boltzmann factor, the density matrix elements (in the Schrödinger representation) for the vibronic states belonging to the $N$ manifold initially after the pulse is turned off are given by

$$p_{\alpha'\beta'}(\tau) = \sum_\alpha p_\alpha E(\omega_{\alpha\alpha'})E(\omega_{\alpha\beta'}) \times \exp(i\omega_{\alpha'\beta'}\tau)\langle\alpha|\alpha'\rangle\langle\alpha|\beta'\rangle, \tag{43}$$

where $E(\omega)$ is the amplitude of the field at frequency $\omega$. In addition to creating vibrational populations in the $N$ manifold ($\alpha' = \beta'$), two types of coherences arise from ths second-order treatment. The first involves electronic coherences between the ground and neutral excited states. This optical coherence will be assumed to decay rapidly and will not be treated explicitly. The second type of coherence comes from the simultaneous excitation of two or more vibrational levels in $N(\alpha' \neq \beta')$. This is possible only if the pulse width is short compared to the period of vibrational motion in the reactant well. Note that although we neglect dissipative effects while the field is turned on, we do allow for free motion of the system due to $H_S$. Note also that the details of the pulse shape do not matter in our approximation, only the pulse area. For the simulations discussed in the next section, we choose the pulse to have a Gaussian temporal profile (and, hence, a Gaussian spectral profile) with a full width half-maximum given by $1/\tau$. We choose the density matrix after excitation to be normalized i.e., $\mathrm{Tr}\rho(\tau) = 1$. For convenience we choose to generate the initial condition using the displaced oscillator states since we assumed that only the $N$ state is coupled to the radiation field. The initial condition (i.e., after the pulse is turned off) in the eigenstate representation can then be generated using the same transformation as in Eq. (34c),

$$\rho(\tau) = \mathbf{U}_{ge}^\dagger \mathbf{U}_{gd} p_d(\tau) \mathbf{U}_{gd}^\dagger \mathbf{U}_{ge}, \tag{44}$$

where $d$ denotes the displaced oscillator representation.

### 3. Numerical solution of the Redfield equations

We take the number of vibrational states in each well to be $N$. The total number of excited vibronic states in our model is thus $2N$. The number of states used in a dynamical calculation depends on the strength of the vibronic coupling parameters ($g_i$), the electronic coupling strength ($J$), and the temperature. We reformulate Eq. (40) such that $\rho$ is a vector of length $(2N)^2$ whose elements contain the populations of and coherences between the system eigenstates. In this notation, $\mathbf{L}$ is $(4N^2 \times 4N^2)$ matrix. Solution of the coupled Redfield equations can then be obtained through numerical matrix diagonalization. We write the solution in the form

$$\rho(t) = \mathbf{M}\exp[\lambda(t-\tau)]\mathbf{M}^\dagger\cdot\rho(\tau), \tag{45}$$

where $\rho(\tau)$ is the density matrix initially after the excitation pulse. $\mathbf{M}$ is the eigenvector matrix of the matrix $\mathbf{L}$, and $\lambda$ is the diagonal matrix of complex-valued eigenvalues. The structure of $\mathbf{L}$ is such that the real part of $\lambda$ is negative.

We are interested in the populations of the $N$ and CT states as a function of time. Thus at each time point we transform back to the displaced oscillator representation to give the density matrix $\mathbf{p}_d(t)$.

$$\mathbf{p}_\mathbf{d}(t) = \mathbf{U}_{gd}^\dagger \mathbf{U}_{ge}\rho(t)\mathbf{U}_{ge}^\dagger \mathbf{U}_{gd}. \tag{46}$$

The total population $P_i$ in site state $i$ is obtained by performing a partial trace over only those vibrational states belonging to state $i$.

$$P_i(t) = \mathrm{Tr}_i\{\mathbf{p}_d(t)\}. \tag{47}$$

To summarize, we transform, using the appropriate unitary matrices, the system states and the fluctuation matrix elements to the eigenstate representation. We next construct the Redfield tensor from the fluctuation matrix elements and solve for the dynamics via numerical diagonalization of the systems Green's function. Finally we transform back to the representation of displaced site states to calculate the population dynamics. This procedure provides a convenient method for simultaneously treating both the coherent processes arising from the optical preparation of the initially excited state and the coupling between the $N$ and CT states.

It is interesting to compare the picture of ET that the different representations provide. In the localized, displaced oscillator representation, a vibronic coherence induced by the electronic coupling parameter $J$ involving both the $N$ and CT states appears as coherent transfer of an electron between the two states. In the delocalized eigenstate representation, this process is the oscillation of a phase coherence at its Bohr frequency between two states that have projections onto both the $N$ and CT manifold. The dephasing of this coherence results in irreversibility of the electron transfer.

Dynamical simulations discussed in Sec. III were carried out on the Cray Y MP at the National Center for Supercomputing Applications at the University of Illinois. The various transformation matrices were obtained from numerical diagonalization of the appropriate Hamiltonian matrices using routines from the I.M.S.L. (Version 10) package. Typical calculations of the dynamics for a two electronic state–one mode model required between 5 and 10 vibronic states per well to achieve convergence.

## III. RESULTS AND DISCUSSION

### A. Weak electronic coupling

For sufficiently weak electronic coupling, the multilevel theory discussed in the previous section should reproduce the golden rule result for the electron transfer rate constant. In this regime the coherence time between vibronic levels is much shorter than the timescale of electronic tunneling, so the process is considered incoherent. Consequently, the golden rule rate for a multilevel system can be obtained by summing all possible pairwise rates for the different vibronic levels.

$$k_{GR} = J^2 \sum_{\alpha'} p_{\alpha'} \sum_{\beta'} |\langle \alpha'_N | \beta'_{CT} \rangle|^2 \left\{ \frac{\Gamma_{\alpha'\beta'}}{(E_{\alpha'} - E_{\beta'})^2 + \Gamma^2_{\alpha'\beta'}} \right\}, \tag{48}$$

where $\alpha'$ and $\beta'$ now refer to vibrational levels belonging to the $N$ and CT states, respectively. $(E_{\alpha'} - E_{\beta'})$ is the detuning between levels and $\Gamma_{\alpha\beta}$ $(= 1/T_2)$ is the total dephasing rate for levels $\alpha'$ and $\beta'$. The use of the Boltzmann factor in the summation over the $N$ manifold assumes that the system is in thermal equilibrium. Slow energy relaxation can result in "hot" transfer between levels but a rate description is still valid. In this case, though, the initial state distribution becomes time-dependent and nonexponential kinetics result.

In this section we wish to investigate the various ways in which the golden rule description can break down, which are related to the persistence of phase coherence and/or incomplete thermalization in the reactant or product well.[20] In what follows we discuss the validity of Eq. (48) starting with the diabatic (site) states, since this represents the starting point for most analyses of electron transfer rates.[36]

The simplest model we can use to illustrate the equivalence of the Redfield theory and the standard golden rule description in a weakly coupled system is a three-level system in which the reactant manifold consists of a single level with the product containing two levels, corresponding to a ground and excited vibrational state. This is illustrated in Fig. 2. The surface parameters and excitation condition are listed in the figure caption and have been chosen so that the three levels shown are the only relevant ones. Here the vibrationally excited state of the product acts as the acceptor level and relaxation to the ground level acts as the only dephasing mechanism (i.e., there is no pure dephasing).

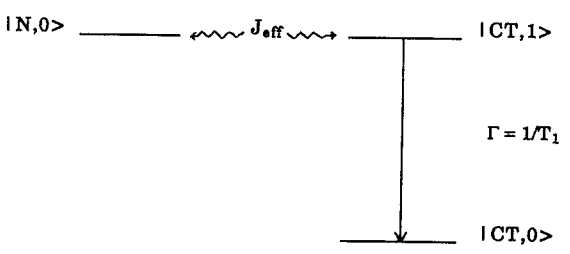


FIG. 2. Schematic diagram of the isolated three-level system described in the text. The potential surfaces are not shown. The parameters are $\omega/2\pi c = 600\ \text{cm}^{-1}$, $g_N/2\pi c = -g_{CT}/2\pi c = -400\ \text{cm}^{-1}$. $J_{\text{eff}}$ is the effective coupling strength, $J_{\text{eff}} = J\langle 0|1\rangle$.

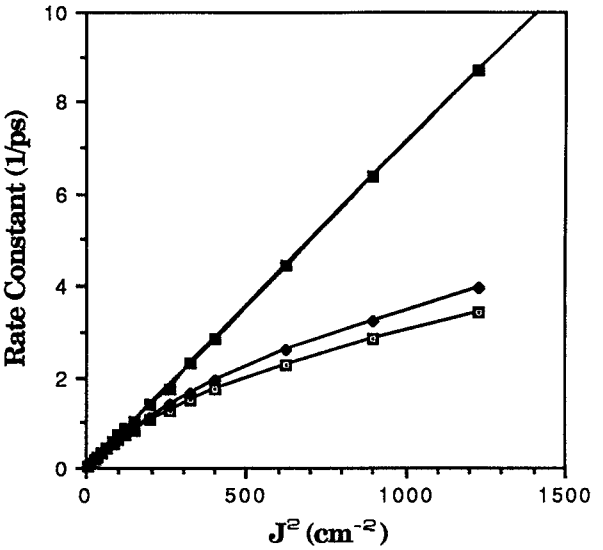


FIG. 3. Electron transfer rate constant as a function of the square of the square of the electronic coupling matrix element, $J/2\pi c$, for the isolated three-level system of Fig. 2. $\epsilon_{\text{bias}}/2\pi c = 100\,\text{cm}^{-1}$. $T_1 = 0.166$ ps, $T_2^* = \infty$. (-■-), golden rule; (-□-), $k_{\text{FP}}$; (-◆-), $k_{\text{AVG}}$.

In our analyses we show the results for both the average rate constant and the rate constant corresponding to the first passage time. These are given by

$$k_{\text{avg}} = \left[ \int_0^\infty dt\, P_N(t) \right]^{-1} \tag{49a}$$

and

$$k_{fp} = (\tau_{fp})^{-1}, \tag{49b}$$

where $\tau_{fp}$ is defined as the time it takes for the population to decay to $1/e$ of its initial value. The population $P_N(t)$ is defined as the population of the $N$ state minus its value at equilibrium. In terms of the density matrix in the site representation this is given by $P_N(t) = p_{NN}(t) - p_{NN}(t = \infty)$. For a multilevel system, $p_{NN}(t)$ is obtained by tracing over the density matrix for the site state $N$. For nonexponential decays, the average time and first passage times will be different.

In the three-level system when there is perfect resonance between the donor and vibrationally excited acceptor level, the golden rule predicts the rate should go as $k_{gr} \sim J^2/\Gamma$, where $\Gamma(= 1/T_1)$ is the vibrational relaxation rate in the present example. Figure 3 shows the results for the electron transfer rate for the three-level system as a function of the square of the electronic coupling strength from both the multilevel Redfield and the golden rule theories for the system described in Fig. 2. As expected, for sufficiently small values of $J$, the results are identical. As the electronic coupling is increased, the calculated rate falls off from the golden rule prediction due to coherent effects (*vide infra*).

Another prediction from the golden rule result is that for cases where there is a detuning between the donor and acceptor levels, the rate constant should depend nonmonotonically on the dephasing rate $\Gamma$. The reason for this is that the fluctuations in the system energy levels induced by the

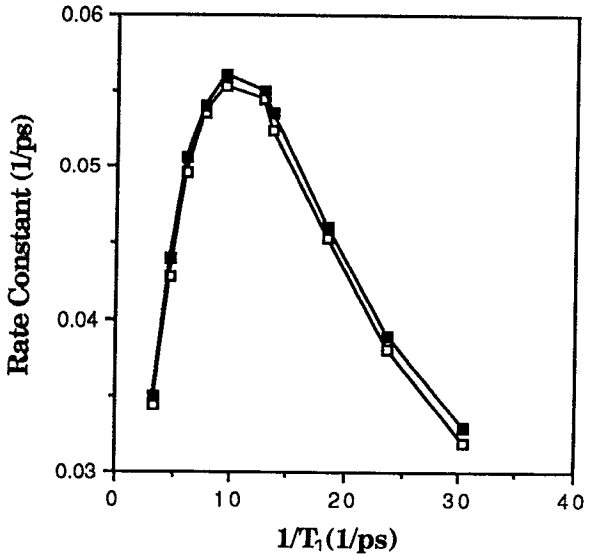


FIG. 4. Electron transfer rate constant as a function of the vibrational relaxation rate, $1/T_1$, for the isolated three-level system. $T_2^* = \infty$. $J/2\pi c = 5.0$ $cm^{-1}$ (-■-), golden rule; (-□-), $k_{AVG}$.

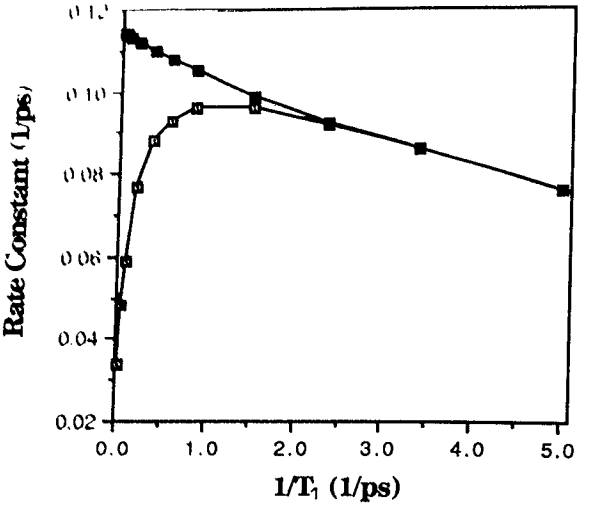


FIG. 5. Electron transfer rate constant as a function of the vibrational relaxation rate, $1/T_1$, for the isolated three-level system. $T_2^* = 0.21$ ps, $J/2\pi c = 5.0\,cm^{-1}$. (-■-), golden rule; (-□-), $k_{FP}$. The average rate is indistinguishable from the first passage rate.

system–bath coupling must have a magnitude large enough to allow states to achieve resonance so that electron transfer can occur. If the magnitude of the energy gap fluctuation is comparable to or less than the detuning, the rate at which the donor and acceptor levels come into resonance is rate controlling. At higher values of the magnitude of the fluctuations, sampling of the resonance condition is no longer rate limiting and the rate turns over. As discussed in Sec. II C, the vibrational relaxation rate is proportional to the magnitude of the mean-square amplitude of the off-diagonal fluctuation constant and provides a convenient parameter with which to investigate the interplay between coherent transfer and energy fluctuations. Figure 4 shows the Redfield and golden rule rates as a function of the vibrational relaxation rate for the three-level system of Fig. 2 with a detuning of $\delta = 25\,cm^{-1}$ and an electronic coupling of $J = 5\,cm^{-1}$. For this case the turnover occurs at $T_1 \approx 0.10$ ps.

The examples above serve to show the equivalence of the Redfield theory and golden rule results for a simple model where the electronic coupling is weak. We now wish to discuss the various ways in which Eq. (48) can break down in both a three-level model and a multilevel system in which both donor and acceptor contain many vibrational states. The deviation from the golden rule result at large values of $J$ seen in Fig. 3 results from the presence of a vibronic phase coherence between levels belonging to different site states. As stated before, the initial condition was chosen such that only the donor site level was populated. In the eigenstate representation, this corresponds to a superposition of the two delocalized (exciton) states with a definite phase relationship between their wave functions. The phase factor is such that there is perfect constructive interference at the donor site and perfect destructive interference at the acceptor site. In the absence of any dephasing mechanism this phase coherence will oscillate at a frequency of $J_{eff}$, where $J_{eff}$ is the bare electron tunneling matrix element dressed by the appropriate Franck–Condon factor. In the site representation this phase rotation will appear as cycling of the population between reactant and product and would be detectable in an optical experiment as a quantum beat. In a dissipative environment, pure dephasing and population relaxation lead to destruction of the initial electronic coherence resulting at long times in a rate-like description. At sufficiently short times, however, the decay of the initial state is not exponential and the coherent aspect of the motion results in an induction period, i.e., the initial slope at $t = 0 \rightarrow 0$. Here the interplay between coherent motion and relaxation leads to a decrease in the actual rate as compared to the golden rule prediction.

In our model, the bias between the ground state levels of the reactant and product is approximately equal to the vibrational frequency. Such a situation leads to a second cause for the breakdown of the golden rule which is due to slow thermal equilibration in the reactant and/or product manifolds. To illustrate this quantitatively, we choose the parameters such the total dephasing rate is much faster than the electron transfer rate and investigate the effects of varying the population relaxation rate of the acceptor for the case where there is no detuning. The results are shown in Fig. 5. Here the diagonal fluctuation constant has been chosen such that the pure dephasing time for the relevant levels is approximately 0.20 ps and the vibrational $T_1$ time is varied from infinity to $\approx 0.10$ ps. For values of $T_1$ less than approximately 1 ps, the rate actually decreases with increasing $T_1$ in contrast to the golden rule prediction based on total dephasing rate. The falloff from the golden rule prediction in this case arises from incoherent recrossings of the intersection region of the two diabatic surfaces. The product manifold can not dump its energy to the ground state and "hot" transfer back to the reactant state can occur. The important point here is that the golden rule theory depends only on the total dephasing rate

without regard to how dephasing is partitioned between population relaxation and pure dephasing. Of course, if we were to turn off the vibrational relaxation rate ($T_1 = \infty$) and consider the isolated two-level system (with $\Delta G = \delta$ rather than $\epsilon_{\text{bias}}$), we would get perfect agreement between the Redfield and golden rule results due to the rapid pure dephasing.

The isolated three-level system discussed above served to demonstrate the validity of the Redfield theory in the limit of very weak coupling and explore two ways in which the golden rule can break down which are due to coherent and incoherent motion of the system through the region where the diabatic surfaces cross. In a system with a low frequency mode and high temperature, the presence of many vibrational levels can lead to complicated dependence of the dynamics on the magnitude and various types of coupling and dissipation in the system. We next examine a series of models designed to explore some of the consequences of the competition between coherent motion and relaxation in a multilevel system. As before we choose the model such that the reaction is exothermic by approximately one quantum of vibrational energy. When the reactant state contains more than one vibrational level, a sufficiently short excitation pulse can result in a vibrational coherence between two or more vibrational levels within the reactant manifold. Such a coherence is reflected in a value of the ensemble-averaged coordinate, $\langle Q(t) \rangle$, that differs from the equilibrium value of $\langle Q \rangle$ corresponding to the photoexcited state (i.e., $\Delta_N$). In order to properly incorporate the magnitude of this initial coherence into our description of the excited state dynamics of our model, we must specify both the position of the $N$ diabatic surface relative to that of the ground state and the spectral width of the excitation pulse. In all cases discussed here, we choose the temporal width to be short enough such that we can neglect dissipation during the pulse. The spectral width is taken to be Gaussian and is obtained from the temporal width, also taken to be Gaussian, by the Fourier transform relation $\tau \cdot \Delta\omega_L \approx 15\ \text{cm}^{-1}$, where $\tau$ and $\Delta\omega_L$ refer to the fullwidth at half-maximum of the temporal and spectral profiles, respectively.

The first issue we examine is the effect of level detunings on the dynamics of ET. Figure 6 shows plots of the rate constant for various electronic coupling values for a multilevel system in which $\hbar\omega \sim kT$. The parameters are chosen so that the reaction falls in the Marcus inverted region[3] and are displayed in the appropriate figure captions. In Fig. 6(a) the reaction is exothermic by precisely one quantum of vibrational energy so that each donor vibronic level is in perfect resonance with an acceptor level. In Fig. 6(b), the levels have been detuned by one-fourth the vibrational frequency. In both cases negative deviations (i.e., slower rates) from the golden rule prediction are seen, and, above a critical value of $J$, nonexponential kinetics are observed; however, in the detuned case the first passage time is shorter than the average lifetime whereas the opposite relation holds for the case of exact resonance. Examples of the population dynamics for different values of the electronic coupling are shown for these two cases in Fig. 7. These decay curves show that for a given value for the total dephasing rate, the onset of coherent behavior occurs at lower values of $J$ for the resonance case

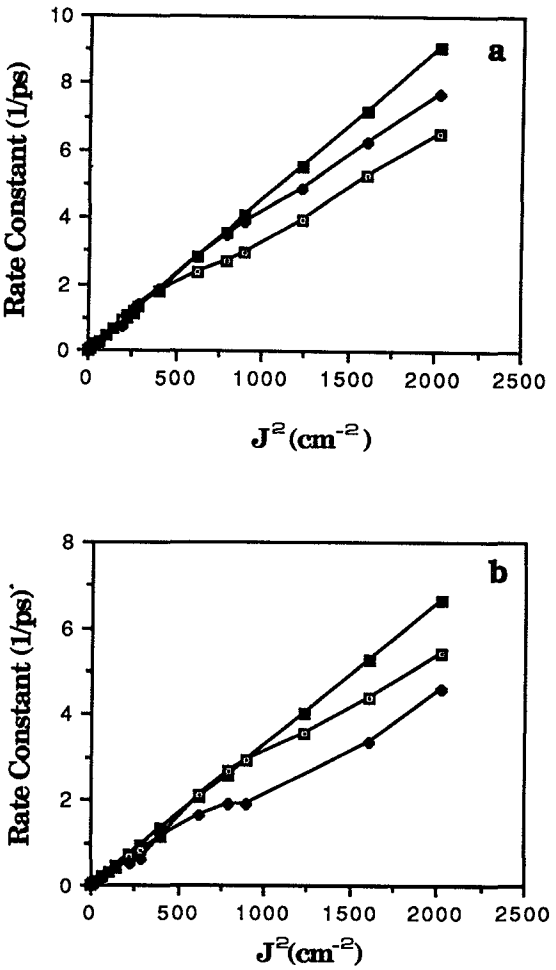


FIG. 6. Electron transfer rate constant as a function of the square of the electronic coupling matrix element for a multi-level system with $\omega/2\pi c = 100\ \text{cm}^{-1}$, $g_N/2\pi c = -g_{CT}/2\pi c = 50\ \text{cm}^{-1}$, $f_1^2/2\pi c = f_2^2/2\pi c = 16.0\ \text{cm}^{-1}$. $(\omega_{\text{exc}} - E_{0-0})/2\pi c = 25\ \text{cm}^{-1}$, $\tau = 0.05$ ps, $T = 200$ K (-■-), golden rule; (-□-), $k_{\text{FP}}$; (-◆-), $k_{\text{AVG}}$. (a) $\epsilon_{\text{bias}}/2\pi c = 100\ \text{cm}^{-1}$. (b) $\epsilon_{\text{bias}}/2\pi c = 125\ \text{cm}^{-1}$.

than for the detuned case. In Fig. 6(b), the decay curves for the faster processes are markedly nonexponential due to the small energy gap for the reaction (compared to $kT$) and the reversible nature of the process. Simulations using the same parameters with a larger energy gap (not shown) yielded decays that were single exponential.

The results above are in agreement with the results seen in the isolated three-level system, in which only negative deviations from the golden rule were seen. The preservation of electronic phase coherence on a sufficiently long time scale compared to the reaction time is responsible for the overestimation of the golden rule result. We next ask if there is any circumstance in which we might expect to see positive deviations from the golden rule prediction, that is, an enhancement of the rate. To answer this, consider the effective coupling strength as a function of vibrational quantum number. In the vicinity of the activationless region, the effective coupling strength ($J_{\text{eff}} = J\sqrt{F}$; $F =$ Franck–Condon fac-

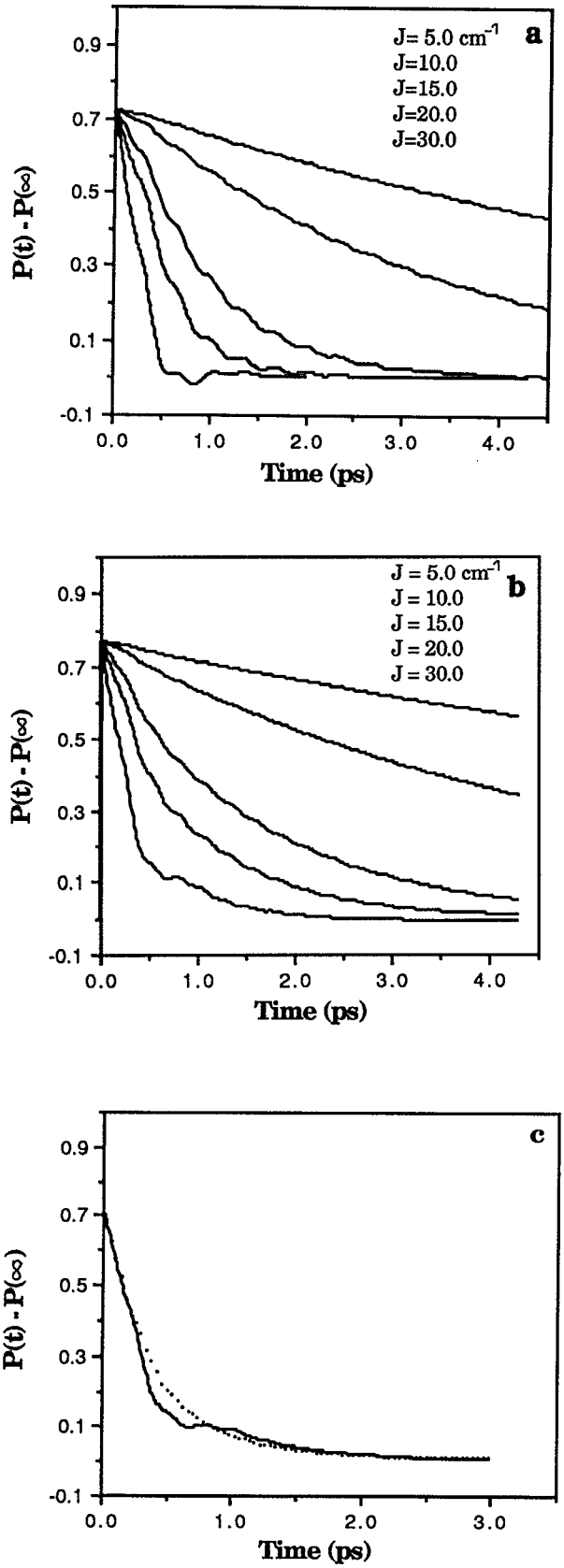


FIG. 7. Population dynamics for the initially excited neutral electronic state for the multilevel system described in Fig. 6. (a). $\epsilon_{bias}/2\pi c = 100\ cm^{-1}$. (b) $\epsilon_{bias}/2\pi c = 125\ cm^{-1}$. (c) (—) $\epsilon_{bias}/2\pi c = 125\ cm^{-1}$, $J/2\pi c = 30\ cm^{-1}$; (···) $\epsilon_{bias}/2\pi c = 225\ cm^{-1}$, $J/2\pi c = 42\ cm^{-1}$.

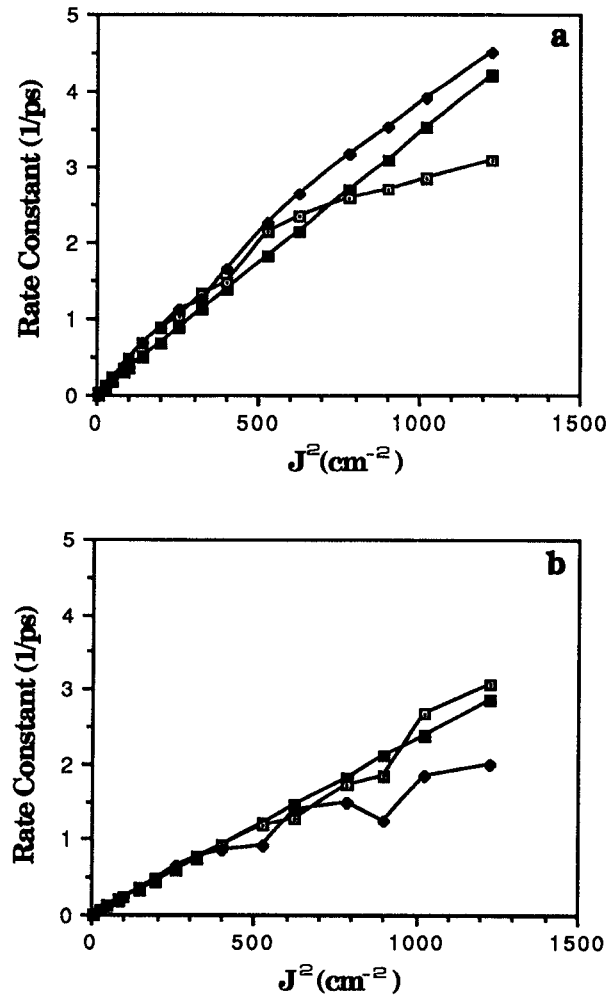


FIG. 8. Electron transfer rate constant as a function of the square of the electronic coupling matrix element for a multilevel system with $\omega/2\pi c = 100\ cm^{-1}$, $g_N/2\pi c = -g_{CT}/2\pi c = 25\ cm^{-1}$, $f_1^2/2\pi c = f_2^2/2\pi c = 16.0\ cm^{-1}$, $(\omega_{exc} - E_{0-0})/2\pi c = 200\ cm^{-1}$, $\tau = 0.05$ ps, $T = 150$ K. (-■-), golden rule; (-□-), $k_{FP}$; (-◆-), $k_{AVG}$. (a) $\epsilon_{bias}/2\pi c = 100\ cm^{-1}$. (b) $\epsilon_{bias}/2\pi c = 125\ cm^{-1}$.

tor) decreases with increasing vibrational quantum number. Thus for a situation in which many donor levels are initially populated, slow energy flow between the reaction coordinate and the surroundings results in depletion of lower vibrational levels of the donor and a slowing of the overall rate. This would suggest that in a situation in which ET from higher vibrational levels of the donor occured with a faster rate than for lower levels, slow energy flow would result in a faster rate than that predicted from a donor that was in thermal equilibrium. Figure 8 shows just a case. Here, the displacement between the reactant and product surfaces is small, and we are in the Marcus inverted region. For the case where there is an exact resonance between donor and acceptor levels there is a slight enhancement of the average rate over the golden rule prediction. When the levels are detuned [Fig. 8(b)], we again see negative deviations from the golden rule. For $J > 100\ cm^{-1}$ we see that the first passage time is faster than the golden rule prediction, however, in this region, recur-

rences are seen in the population dynamics and direct comparison with the golden rule is meaningless.

The simulation results from these models are not meant to suggest universal behavior, rather they serve to illustrate some qualitative points concerning the complexities that arise when vibrational population dynamics, dephasing and ET processes occur on similar timescales. From the examples above, it was seen that under the right combination of circumstances, such as small displacements between reactant and product wells coupled with slow energy exchange with the bath, rates exceeding the golden rule prediction could be realized. Of course the golden rule formula could be modified to include a time-dependent distribution in the reactant well. If pure dephasing were rapid, then the decay of the population in the reactant well could be calculated by solving the full multilevel Pauli master equation using the state-to-state rates calculated as in Eq. (48). This presumably would lead to the same results as those from Redfield theory.

In the isolated three-level system we found that when the electronic coupling matrix element approached the value of the population relaxation rate, the short time behavior of the population of the initial state was found be coherent [i.e., $P(t) \sim \cos(4\pi Jt)$] which resulted in an increase in the first passage time and decrease in the average rate constant compared to that predicted by the golden rule. It is not clear, however, how this idea translates into the multilevel case where each pair of quasiresonant levels in the reactant and product has its own effective frequency of oscillation. From the limited number of cases we have examined we conclude there is no *general* statement that can be made concerning positive or negative deviations from golden rule behavior due to coherence effects in a multilevel system. In the cases studied here, the fluctuation parameters were identical in each well. The results obtained suggest that in these cases, strong coherences lead to negative deviations from the golden rule result while slow energy flow between system and bath could lead to positive or negative deviations depending on how Franck–Condon factors scale with vibrational energy.

Another issue is the effect of the initial optical excitation. Whether or not deviations from the golden rule prediction are seen may depend on both the magnitude of the initial vibrational coherence and the amount of excess vibrational energy deposited in the reactant well during the excitation process. We next examine the role of the nature of the optically prepared state on the subsequent dynamical behavior of the system. The two models we compare differ only in the position of the ground state relative to the $N$ state. The essential difference between the two models is the difference in the Franck–Condon factors for the initial excitation process. A larger displacement of the $N$ state from the ground state results in a greater number of vibronic states that are initially accessible. In addition, we have chosen the excitation condition such that the center frequency of the excitation pulse is approximately in resonance with the $0 \rightarrow 5$ transition for the case where the displacement of the $N$ state is large. For the smaller displacement case, the spectral center of the excitation is in resonance with the $0 \rightarrow 1$ band. In both cases the

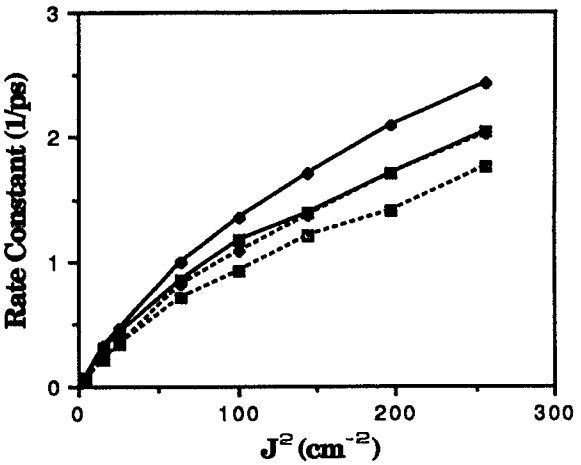


FIG. 9. Electron transfer rate constant as a function of the square of the electronic coupling matrix element for a multilevel system with $\epsilon_{bias}/2\pi c = \omega/2\pi c = 100\,cm^{-1}, f_1^2/2\pi c = 1.0\,cm^{-1}, f_2^2/2\pi c = 16.0\,cm^{-1}, T = 150$ K, $\tau = 0.05$ ps. The solid lines refer to the case where $g_N/2\pi c = -g_{CT}/2\pi c = -40\,cm^{-1}$ and $(\omega_{exc} - E_{0-0})/2\pi c = 15\,cm^{-1}$. The dashed lines refer to the case where $g_N/2\pi c = -80\,cm^{-1}$, $g_{CT}/2\pi c = 0\,cm^{-1}$, and $(\omega_{exc} - E_{0-0})/2\pi = 500\,cm^{-1}$. (-■-, -□-) $k_{FP}$; (-◆-, -◇-), $k_{AVG}$.

temporal width of the excitation pulse was taken to be 0.050 ps corresponding to a spectral width of approximately 300 $cm^{-1}$. The combination of different displacements and different excitation conditions results in initial conditions which are quite different from one another. We now examine the dynamics for these two situations in the presence of different dissipative mechanisms. Figure 9 shows the results for the two models for the case where there is relatively fast vibrational energy equilibration and slow pure dephasing. The rate constants obtained for the different initial condi-

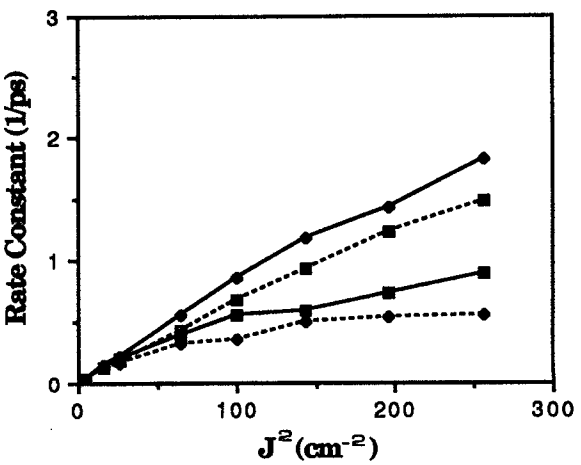


FIG. 10. Electron transfer rate constant as a function of the square of the electronic coupling matrix element for a multilevel system with $\epsilon_{bias}/2\pi c = \omega/2\pi c = 100\ cm^{-1}$, $f_1^2/2\pi c = 2.85\ cm^{-1}$, $f_2^2/2\pi c = 1.4\ cm^{-1}$, $T = 150$ K. $\tau = 0.05$ ps. The solid lines refer to the case where $g_N/2\pi c = -g_{CT}/2\pi c = -40\,cm^{-1}$ and $(\omega_{exc} - E_{0-0})/2\pi c = 15\,cm^{-1}$. The dashed lines refer to the case where $g_N/2\pi c = -80\ cm^{-1}$, $g_{CT}/2\pi c = 0\,cm^{-1}$ and $(\omega_{exc} - E_{0-0})/2\pi c = 500\,cm^{-1}$. (-■-, -□-) $k_{FP}$; (-◆-, -◇-), $k_{AVG}$.

tions are different with the difference increasing with increasing values of the electronic coupling strength. A similar situation is shown in Fig. 10, however this time the pure dephasing rate is chosen to be rapid while the vibrational $T_1$ time is relatively slow. The discrepancy between first passage times and between average rates for the two models is greater in the case of slow energy equilibration than for fast equilibration indicating the effect of hot transfer out of the donor state. In addition, the difference between the average and first passage rates for both models is substantially greater in the case of slow energy flow.

### B. Comparison with semiclassical theory

When the barrier between the reactant and product surfaces is large and/or the temperature is high, nuclear tunneling has little or no effect on the dynamics and the reaction can be described as activated barrier crossing. In this case classical or semiclassical treatments are valid. In the semiclassical Landau–Zener theory, motion of the system along the reaction coordinate is treated classically, except at the crossing point of the diabatic surfaces where the Schrödinger equation is used to solve for the probability for the system to "hop" from the reactant diabatic surface to that of the product. In its simplest form, Landau–Zener theory treats the motion through the crossing point ballistically. The probability of reaction occurring on a single passage through the crossing point is given by

$$P_{LZ} = 1 - \exp(-2\pi J^2/hv|\Delta F|), \tag{50}$$

where $v$ is the velocity of the system at the crossing and $|\Delta F|$ is the absolute value of the difference in slopes of the diabatic surfaces at the intersection. The ballistic version of Landau–Zener theory should be most appropriate in the nonadiabatic limit. Here the barrier is cusp-like and the assumption of ballistic motion near the crossing point would seem to be reasonable. The reasoning behind this is due to Frauenfelder and Wolynes who discuss the effects of friction in Landau–Zener theory using length scale arguments.[15] The Landau–Zener length is defined as

$$l_{LZ} = \frac{2J}{|\Delta F|}. \tag{51}$$

This is essentially the region in which lower adiabatic surface is within an energy $2J$ of the barrier. A second length scale can be defined by replacing $2J$ by kT. This is the region of the lower adiabatic surface in which the upper surface is thermally accessible and is known as the transition state length scale.

$$l_{TS} = kT[|F_N|^{-1} + |F_{CT}|^{-1}]. \tag{52}$$

The final length scale of interest is the mean free path of the reaction coordinate which is related to the classical friction coefficient, $\zeta$ by

$$\lambda = \sqrt{(2mkT)}/\zeta. \tag{53}$$

It turns out that if the Landau–Zener length satisfies the relation

$$l_{LZ} \ll l_{TS} \ll \lambda, \tag{54}$$

then to a good approximation the rate constant is given by the transition state theory result times the Landau–Zener probability [Eq. (50)]. Thus in the strongly nonadiabatic regime, the rate constant for ET is given by

$$k = [1 - \exp(-2\pi J^2/hv_T|\Delta F|)] \times (\omega/2\pi)\exp(-E_B/k_BT), \tag{55}$$

where $v_T$ is the thermal velocity ($=\sqrt{kT/\pi m}$; $m=1$ in dimensionless units). As the electronic coupling is increased, the barrier becomes more dome-like, the Landau–Zener length becomes comparable to, or greater than, the mean free path and/or transition state lengths and the motion in the vicinity of the barrier is diffusive on any relevant length scale.

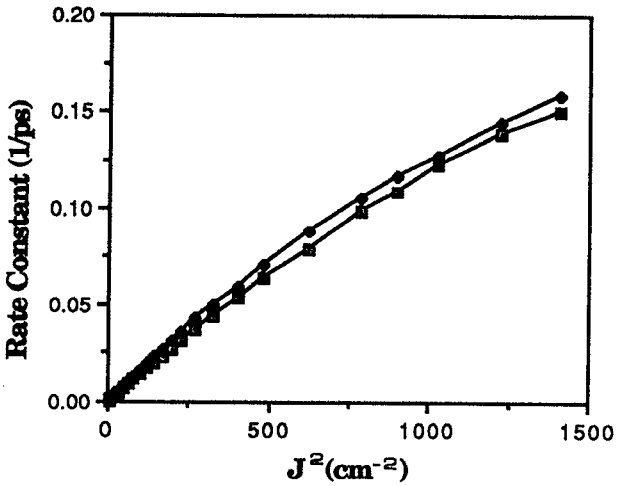


FIG. 11. Comparison of Redfield and Landau–Zener rates for a multilevel system with $\epsilon_{bias}/2\pi c = 0$ cm$^{-1}$, $\omega/2\pi c = 100$ cm$^{-1}$, $g_N/2\pi c = -g_{CT}/2\pi c = 145$ cm$^{-1}$, $f_1^2/2\pi c = 2.75$ cm$^{-1}$, $f_2^2/2\pi c = 49.0$ cm$^{-1}$, $T = 298$ K, $(\omega_{exc} - E_{0-0})/2\pi c = 0$ cm$^{-1}$, $\tau = 0.20$ ps. (-□-), Redfield theory; (-◆-), Landau–Zener theory.

A systematic comparison of the multilevel Redfield theory with Landau–Zener over a wide range of coupling strengths would require forging a connection between the concept of friction and the fluctuation parameters of our quantum model. This will be discussed in a future work. We can skirt this issue by working in the weak coupling limit. We choose our fluctuation constants somewhat arbitrarily such that the relaxation times are such that Eq. (54) is satisfied. In this region the dynamics turn out to be rather insensitive to the exact values for $T_1$ and $T_2^*$. For higher values of the relaxation rates, the assumption of a mean free path for the reaction coordinate that is long compared to the Landau–Zener length would appear to be invalid. A comparison of the results for the rate constant from the Redfield and Landau–Zener theory in the nonadiabatic limit is shown in Fig. 11. The parameters are listed in the caption. The results are in good agreement and suggest that the multilevel quantum theory described here will be useful in providing a unified description of ET over a wide range of temperatures and coupling strengths.

### C. Weak damping limit

As discussed earlier, coherent excitation of the $N$ state manifold with a laser pulse satisfying $\tau \ll \omega^{-1}$ results in a

vibrational phase coherence between several levels. This coherence can interfere with the reversible ET process leading to complicated dynamical behavior giving rise to quantum beats. Dephasing smears out this interference effect and, for fast enough dephasing, results in a monotonic, irreversible loss of population from the initially excited manifold. In this section we show results for multilevel systems in which there is little or no dephasing. While this section is meant to illustrate the effects of various types of coherences that are created in a short pulse experiment, the results will possibly provide insight into experiments carried out at very low temperature where dephasing times can be quite long. Such a situation has recently been observed in the short-time dynamics following excitation into the primary-donor state of the reaction center of the photosynthetic bacterium Rb, sphaeroides.[37] Quantum beats suggested to originate from a vibrational coherence involving the reactive degree of freedom were seen in transient absorption experiments over a broad temperature range.

An excellent observable for understanding the interplay between various types of coherences in a complicated multilevel system is the ensemble-averaged value of the reaction coordinate operator given by

$$\langle Q(t)\rangle = \mathrm{Tr}_s\{\mathbf{p}(t)Q\}, \tag{56}$$

where

$$Q = 1/\sqrt{2}\{(a + a^\dagger - \Delta_N)|N\rangle\langle N| + (a + a^\dagger - \Delta_{CT})|CT\rangle\langle CT|\}. \tag{57}$$

The equilibrium value for $\langle Q\rangle$ is thus $\Delta_N$ when the system is in the reactant state and $\Delta_{CT}$ when the system is in the product state. In the presence of an electronic coupling between the two wells, the equilibrium value is

$$\langle Q(t=\infty)\rangle = 1/\sqrt{2}\sum_i \exp(-\beta E_i)\Delta_i/\sum_i \exp(-\beta E_i). \tag{58}$$

A vibronic coherence between two levels in different manifolds will cause $\langle Q(t)\rangle$ to oscillate at a frequency determined by the effective coupling strength. That part of $\langle Q(t)\rangle$ that is due to a vibrational coherence within a single manifold will oscillate at the frequency of the well. This can give rise to some interesting interference effects depending on how the system is prepared. Fig. 12(a) shows results for the time dependence of the ensemble-averaged reaction coordinate, obtained from Eq. (56), and the survival probability for a system which experiences no dissipation. In Fig. 12(a), the solid line corresponds to a case where the excitation is high into the absorption band and has a spectral width of approximately 800 $\mathrm{cm}^{-1}$ resulting in coherent excitation of the entire absorption band. This impulsive excitation results in a large initial coherence which is clearly seen to oscillate at the vibrational frequency. The lower frequency modulation is due to the coherence between reactant and electronic states induced by the electronic coupling. The initial value is $\langle Q(0)\rangle = 0$ corresponding to the ground state average. The dashed line corresponds to a situation where the excitation is centered at approximately the $0\rightarrow 0$ transition and has a spectral width of only 50 $\mathrm{cm}^{-1}$. The resulting vibrational coherence has a substantially smaller magnitude

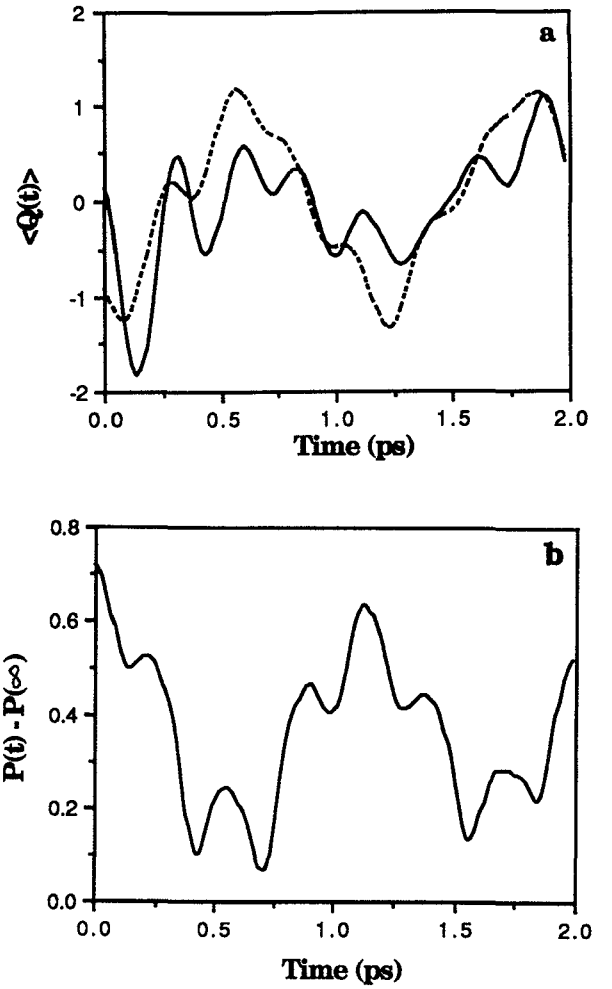


FIG. 12. (a) Ensemble-averaged trajectory for the reaction coordinate for a multilevel system with $\epsilon_{bias}/2\pi c = \omega/2\pi c = 100\ \mathrm{cm}^{-1}$, $J/2\pi c = 30\ \mathrm{cm}^{-1}$, $g_N/2\pi c = -g_{CT}/2\pi c = -75\ \mathrm{cm}^{-1}$, $f_1^2/2\pi c = f_2^2/2\pi c = 0\ \mathrm{cm}^{-1}$, $T = 150$ K. (—) $(\omega_{exc} - E_{0-0})/2\pi c = 350\ \mathrm{cm}^{-1}$, $\tau = 0.02$ ps; (- - - -) $(\omega_{exc} - E_{0-0})/2\pi c = 350\ \mathrm{cm}^{-1}$. $\tau = 0.35$ ps. (b) Corresponding population dynamics of the initially excited neutral state.

and the lower frequency electronic coherence can be clearly seen. The population dynamics in this case is quite complicated due to the participation of many pairs of levels with different effective coupling strengths and is shown in Fig. 12(b). Detuning the donor and acceptor levels by a small fraction of the well frequency has a noticeable effect on the dynamics. Figure 13 shows the results for $\langle Q(t)\rangle$ for the same system as shown in Fig. 12(a) except with a 25 $\mathrm{cm}^{-1}$ detuning. Note in Fig. 13 the trajectory at short time ( $< 1$ ps) is very similar to that seen in Fig. 12(a). The effect of level detuning is seen at longer times after the population has made one round trip between surfaces. In the detuned case this results in a phase shift and some destructive interference after approximately 1 ps.

Finally we show the effect of increasing the dephasing rate on a system with the same parameters as that discussed in Fig. 12, however with a smaller value of the electronic

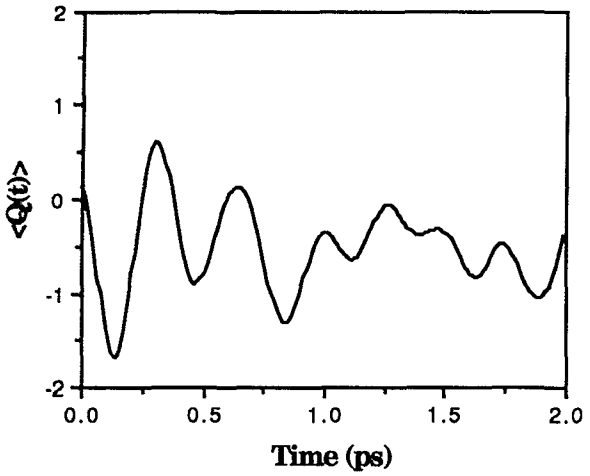


FIG. 13. Ensemble-averaged trajectory for the reaction coordinate for the multilevel system shown in Fig. 12(a) with $\epsilon_{bias}/2\pi c = 125\ cm^{-1}$.

coupling. The results are shown in Fig. 14. The interference between the electronic and vibrational coherences is clearly seen when there is no dephasing. At higher dephasing rates, the system loses all phase information rapidly and the ET process occurs incoherently. In this case, the time dependence of $\langle Q(t) \rangle$ tracks exactly that of the populations of the two states.

## IV. CONCLUSIONS

We have presented a multilevel Redfield theory for treating electron transfer dynamics in a dissipative environment that is valid for arbitrarily large electronic coupling. The major point of this treatment is that by carrying out the dynamics in the representation that diagonalizes the electronic coupling operator we can interpolate between the coherent and incoherent limits for the dynamics. In addition the formalism allows proper incorporation of finite vibrational energy relaxation and dephasing rates into the de-

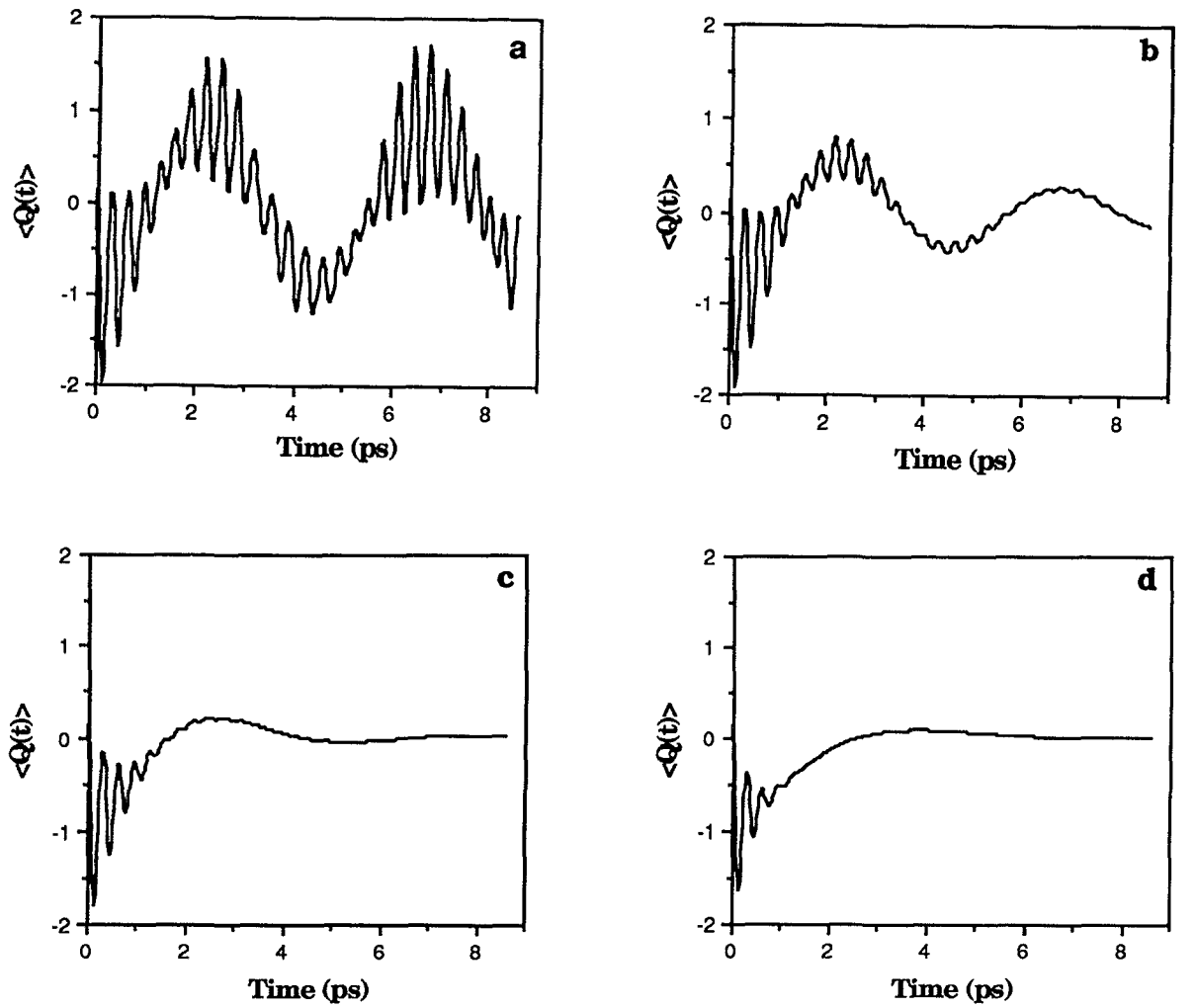


FIG. 14. Ensemble-averaged trajectory for the reaction coordinate for a multilevel system with $\epsilon_{bias}/2\pi c = \omega/2\pi c = 100\ cm^{-1}$, $J/2\pi c = 10\ cm^{-1}$, $g_N/2\pi c = -g_{CT}/2\pi c = -75\ cm^{-1}$, $f_1^2/2\pi c = f_2^2/2\pi c = 0\ cm^{-1}$, $T = 150$ K, $(\omega_{exc} - E_{0-0})/2\pi c = 350\ cm^{-1}$, $\tau = 0.02$ ps. (a) $f_1^2/2\pi c = f_2^2/2\pi c = 0\ cm^{-1}$; (b) $f_1^2/2\pi c = f_2^2/2\pi c = 1.0\ cm^{-1}$; (c) $f_1^2/2\pi c = f_2^2/2\pi c = 24.0\ cm^{-1}$; (d) $f_1^2/2\pi c = f_2^2/2\pi c = 10.0\ cm^{-1}$.

scription of the transfer dynamics.

Comparison of results from a two state–one mode model using a variety of parameter sets demonstrated the equivalence of our method and approaches based on the golden rule of perturbation theory, in cases where nuclear tunneling is important, and the semiclassical Landau–Zener theory in the nonadiabatic limit when electron transfer can be considered a barrier crossing process. The breakdown of the golden rule description due to both finite dephasing rates and slow thermal equilibration in the reactant or product well was investigated in a quantitative manner. Coherence effects were seen to lead to a slower rate than predicted by the golden rule, while slow energy flow between the reaction coordinate and the surroundings were shown to cause positive or negative deviations from the golden rule depending on both the excitation conditions and Franck–Condon effects.

Finally, dynamical simulations of a coupled system in the coherent or weak-damping limit yielded quantum trajectories of the reaction coordinate which were shown to contain information on both electronic and vibrational coherences.

## ACKNOWLEDGMENTS

R.A.F. and G.R.F. would like to thank the DOE and NSF, respectively, for support. R.A.F. is the holder of a Research Career and Development Award and a Camille and Henry Dreyfus Teacher-Scholar. We would also like to thank Professor Robert Silbey for helpful conversations and Professor Mark Ratner for his critical reading of the manuscript.

[1] J. Ulstrup, *Charge Transfer Processes in Condensed Media* (Springer-Verlag, Berlin, 1979).
[2] *Tunneling in Biological Systems*, edited by B. Chance *et al.* (Academic, New York, 1979).
[3] N.Sutin and R. A. Marcus, Biochim. Biophys. Acta **811**, 265 (1985).
[4] K. V. Mikkelsen and M. A. Ratner, Chem. Rev. **87**, 113 (1987).
[5] J. N. Onuchic, D. N. Beratan, and J. J. Hopfield, J. Phys. Chem. **90**, 3707 (1986).
[6] A. Warshel and J.-K. Hwang, J. Chem. Phys. **84**, 4938 (1986).
[7] A. Garg, J. N. Onuchic, and V. Ambegoakar, J. Chem. Phys. **83**, 4491 (1985).
[8] J. T. Hynes, J. Phys. Chem. **90**, 3701 (1986).
[9] E. W. Knapp and S. F. Fischer, J. Chem. Phys. **87**, 3880 (1987).
[10] M. Sparpaglione and S. Mukamel, J. Chem. Phys. **88**, 3263 (1988).
[11] I. Rips and J. Jortner, J. Chem. Phys. **87**, 2090 (1987).
[12] M. Morillo, D. Y. Yang, and R. I. Cukier, J. Chem. Phys. **90**, 5711 (1989).
[13] Y. R. Shen, *The Principles of Nonlinear Optics* (Wiley, New York, 1984).
[14] S. Mukamel, Annu. Rev. Phys. Chem. **41**, 647 (1990).
[15] H. Frauenfelder and P. G. Wolynes, Science **229**, 337 (1985).
[16] R. E. Cline, Jr. and P. G. Wolynes, J. Chem. Phys. **86**, 3836 (1987).
[17] J. E. Straub and B. J. Berne, J. Chem. Phys. **87**, 6111 (1987).
[18] J. Jortner, J. Chem. Phys. **64**, 4860 (1976).
[19] V. G. Levich, Adv. Electrochem. Electrochem. Eng. **4**, 249 (1966).
[20] J. N. Onuchic and P. G. Wolynes, J. Phys. Chem. **92**, 6495 (1988).
[21] J.-L. Martin, J. Breton, A. J. Hoff, A. Migus, and A. Antonetti, Proc. Natl. Acad. Sci. U.S.A. **83**, 957 (1986).
[22] C. Kirmaier and J. D. Holten, FEBS. Lett. **239**, 211 (1988).
[23] G. R. Fleming, J. L. Martin, and J. Breton, Nature **333**, 190 (1988).
[24] C. Lauterwasser, U. Finkele, H. Scheer, and W. Zinth, Chem. Phys. Lett. **183**, 471 (1991).
[25] M. Wasielewski and D. M. Tiede, FEBS Lett. **204**, 368 (1986).
[26] Y. Won and R. A. Friesner, Biochim. Biophys. Acta **977**, 99 (1989).
[27] A. G. Redfield, Adv. Magn. Reson. **1**, 1 (1965).
[28] A. Abragam, *The Principles of Nuclear Magnetism* (Oxford, London, 1961).
[29] P. deBree and D. A. Wiersma, J. Chem. Phys. **70**, 790 (1979).
[30] R. Wertheimer and R. Silbey, J. Chem. Phys. **74**, 686 (1981).
[31] A. J. Leggett, S. Chakravarty, A. T. Dorsey, M. P. A. Fisher, A. Garg, and W. Zwerger, Rev. Mod. Phys. **59**, 1 (1987).
[32] S. Velsko and D. W. Oxtoby, J. Chem. Phys. **72**, 2260 (1980).
[33] J. Chesnoy and G. M. Gale, Adv. Chem. Phys. **LXX**, 297 (1988).
[34] R. Silbey and R. Wertheimer, Chem. Phys. Lett. **75**, 243 (1980).
[35] V. Villaeys and K. F. Freed, Chem. Phys. **39**, 51 (1979).
[36] An obvious, but nevertheless important, point is that the Fermi golden rule is always valid provided one starts from a properly chosen set of zeroth-order states. If coherences exist initially, one could define a new set of states that incorporate these coherences and implement the golden rule formula from this basis. The motivation for discussing our results in the context of the golden rule using localized site states is that this representation is the most natural one for experimentalists to use in thinking about reaction dynamics. In general, one knows something about the level structure, possibly even dynamical quantities such as vibrational dephasing times, in the donor ad/or acceptor species in the absence of the electronic interaction. Of course in the actual computations using Redfield theory, we do work in a representation where the only coupling terms are those between the system eigenstates and the bath, which are considered to be sufficiently weak that second-order perturbation theory (i.e., golden rule) can be used. In this representation, however, coherences still exist initially.
[37] M. H. Vos, J.-C. Lambry, S. J. Robles, D. C. Youvan, J. Breton, and J.-L. Martin, Proc. Natl. Acad. Sci. U.S.A. **88**, 8885 (1991).